32nd URSI GASS, Montreal, 19-26 August 2017

# Characteristic Mode Analysis Enhanced by Reduced-Order Modeling of Arbitrary Background Inhomogeneity

Q. I. Dai(1), H. Gan (1), W. C. Chew(1)
(1) University of Illinois at Urbana-Champaign

## Abstract

We perform characteristic mode analysis (CMA) for objects that are immersed in arbitrary electromagnetic environment where background inhomogeneities are present. Our scheme leverages the reduced modal representation of the numerical Green's function (NGF) to model the scattering effect of the background. The computation of the object-background interaction is expedited with the low-rank randomized singular value decomposition (RSVD) and the discrete empirical interpolation method (DEIM). With the proposed reduced-order modeling, it is feasible to extend CMA to more practical and complicated applications, which offers useful guidance in microwave engineering, such as synthesis of radar cross section (RCS) in inhomogeneous environment.

## 1. Introduction

Characteristic mode analysis (CMA) is a versatile design and analysis tool that gives a systematic and deterministic procedure to determine the electromagnetic properties such as resonances, energy storage and leakage of a structure based on its geometry and material properties [1-3]. In antenna design, it offers valuable insight into the behavior of an antenna irrespective of the arrangement of feed and load, benefiting antenna engineers by offering better understanding of antenna resonances that are judiciously tailored to achieve desired design goals. Advancement of wireless communication technology requests modern antenna systems to properly operation in increasingly complicated environment, such as antennas mounted on an aircraft, and a cell phone placed by a human head or in a car. These applications pose tremendous challenges to the conventional analysis via characteristic modes that is applicable to objects in free space only.

To address this restriction, we present in this paper a novel scheme which empowers CMA with the capability of analyzing conducting objects that are immersed in arbitrary electromagnetic environment. The scheme is formulated on the electric field integral equation (EFIE) where the generalized impedance boundary condition (GIBC) and the numerical Green's function (NGF) are leveraged for the evaluation of the interaction with the background inhomogeneity. It is usually computationally expensive to process with an NGF that corresponds to the inverse of a global finite-element (FE) matrix. We present an efficient reduced modal representation, which offers good approximation to NGFs yet tremendously reduces the model complexity. The NGF can be cheaply evaluated through a small number of physical solenoidal modes, and the solutions to a Poisson's equation as well as a low frequency problem. The low-rank randomized singular value decomposition (RSVD) and the discrete empirical interpolation method (DEIM) are adopted to further reduce the model complexity in modeling complicated object-background interactions. Significantly broadening the applicability of CMA and putting physical insight back into simulation, our reduced order NGF-CMA scheme offers an alternative yet powerful model order reduction tool to the design and analysis of systems interacting with complicated environment.

## 2. Formulation

Consider a general inhomogeneous problem as shown in Fig. 1, where the domain $\Omega_1$ corresponds to the conducting object to be analyzed with the characteristic mode theory, and the domain $\Omega_2$ corresponds to the arbitrary background inhomogeneity.

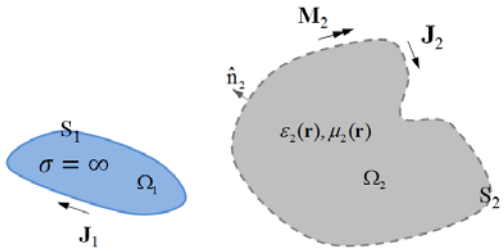


**Figure 1**. A general inhomogeneous electromagnetic problem.

The most critical component in NGF-CMA is to derive the EFIE (electric field integral equation) impedance operator of the conducting object 1. The impedance operator relates the surface current $\mathbf{J}_1$ to the tangent electric field on the surface $S_1$.

To correctly account for the scattering effect of an arbitrary background inhomogeneity 2, we leverage the finite-element (FE) based generalized impedance boundary condition (GIBC) scheme. Consider the incident field generated by the surface current source $\mathbf{J}_1$ that impinges on $S_2$ which is a fictitious surface enclosing $\Omega_2$ .

Assume the equivalence electric and magnetic currents residing on $S_2$ are $\mathbf{J}_2$ and $\mathbf{M}_2$, respectively. The EFIE for inhomogeneity 2 is formulated as

$$\mathcal{L}_{22}(\mathbf{r},\mathbf{r}')\cdot\mathbf{J}_2(\mathbf{r}')-\mathcal{K}_{22}(\mathbf{r},\mathbf{r}')\cdot\mathbf{M}_2(\mathbf{r}')=-\mathcal{L}_{21}(\mathbf{r},\mathbf{r}')\cdot\mathbf{J}_1(\mathbf{r}') \tag{1}$$

where integration is implied with repeated variables. The integral operators are defined as

$$\begin{aligned}\mathcal{L}_{mn}(\mathbf{r},\mathbf{r}')\cdot\mathbf{J}_n(\mathbf{r}')&=i\omega\mu_0\int_{S_n}d\mathbf{r}'\,\overline{\mathbf{G}}(\mathbf{r},\mathbf{r}')\cdot\mathbf{J}_n(\mathbf{r}'),\ \mathbf{r}\in S_m\\ \mathcal{K}_{mn}(\mathbf{r},\mathbf{r}')\cdot\mathbf{M}_n(\mathbf{r}')&=\int_{S_n}d\mathbf{r}'\,\nabla\times\overline{\mathbf{G}}(\mathbf{r},\mathbf{r}')\cdot\mathbf{M}_n(\mathbf{r}'),\ \mathbf{r}\in S_m\end{aligned} \tag{2}$$

Using the FE based GIBC, one can relate $\mathbf{J}_2$ and $\mathbf{M}_2$ as

$$\mathbf{M}_2=\mathcal{Z}_2\cdot\mathbf{J}_2=\hat{n}_2\times ik_0\eta_0\{\mathbf{N}\}^T\cdot[K]^{-1}\cdot\{\mathbf{N}\}\cdot\mathbf{J}_2 \tag{3}$$

where $\mathcal{Z}_2$ is the generalized impedance operator, $\{\mathbf{N}\}$ is the column vector containing all FE vector basis functions in $\Omega_2$ (including $S_2$) as its entries. The FE stiffness-mass matrix is computed as

$$\begin{aligned}[K]_{mn}&=[S]_{mn}-k_0^2[T]_{mn}\\&=\int_{\Omega_2}dV[\mu_{2r}^{-1}(\nabla\times\mathbf{N}_m)]\cdot[(\nabla\times\mathbf{N}_n)-k_0^2\varepsilon_{2r}\mathbf{N}_m\cdot\mathbf{N}_n]\end{aligned} \tag{4}$$

We leverage a novel reduced modal representation of the NGF, which offers an efficient way to compute the inverse of FE matrix as

$$\begin{aligned}[K]_R^{-1}(k)&=[K]^{-1}(k_L)+\left(\frac{1}{k_L^2}-\frac{1}{k^2}\right)[P]\\&+(k^2-k_L^2)[U_s]\cdot\left(k_L^2[I]-[\Lambda]\right)^{-1}\cdot\left(k^2[I]-[\Lambda]\right)^{-1}\cdot[U_s]^{\mathrm{T}}\end{aligned} \tag{5}$$

where

$$[P]=[G]\cdot\left([G]^{\mathrm{T}}\cdot[T]\cdot[G]\right)^{-1}\cdot[G]^{\mathrm{T}} \tag{6}$$

In the above, $[G]$ is the sparse gradient matrix, $[U_s]$ is a matrix containing a small number of low-order solenoidal modes as its columns, $[\Lambda]$ is a diagonal matrix containing the square of wavenumbers of solenoidal modes, $[I]$ is an identity matrix, and $k_L$ is a predefined low wavenumber [4]. In the above, the sparse LU decomposition of $[K]^{-1}(k_L)$ is precomputed and stored, $[P]$ is precomputed by solving a Poisson's equation, $[U_s]$ and $[\Lambda]$ are precomputed by solving a generalized eigenvalue problem. When the frequency varies, the NGF can be obtained immediately with the broadband expression (5). They can also be reused as the geometry of $S_1$ varies.

The surface current $\mathbf{J}_2$ is therefore computed as

$$\mathbf{J}_2=-\left[\mathcal{L}_{22}-\mathcal{K}_{22}\cdot\mathcal{Z}_2\right]^{-1}\cdot\mathcal{L}_{21}\cdot\mathbf{J}_1 \tag{7}$$

And the field generated by $\mathbf{J}_2$ and $\mathbf{M}_2$ that impinges on $S_1$ is

$$\mathcal{L}_{12}\cdot\mathbf{J}_2-\mathcal{K}_{12}\cdot\mathbf{M}_2=\left(\mathcal{L}_{12}-\mathcal{K}_{12}\cdot\mathcal{Z}_2\right)\cdot\mathbf{J}_2 \tag{8}$$

Including the perturbation (scattering) part contributed from the background inhomogeneity 2, the EFIE impedance operator for object 1 is modified as

$$\mathcal{L}_{1,\mathrm{EFIE}}=\mathcal{L}_{11}-\left(\mathcal{L}_{12}-\mathcal{K}_{12}\cdot\mathcal{Z}_2\right)\cdot\left[\mathcal{L}_{22}-\mathcal{K}_{22}\cdot\mathcal{Z}_2\right]^{-1}\cdot\mathcal{L}_{21} \tag{9}$$

Therefore, the characteristic mode formulation of object 1 can be formulated as [1]

$$\mathcal{X}_{1,\mathrm{EFIE}}\cdot\mathbf{J}_1=\lambda\mathcal{R}_{1,\mathrm{EFIE}}\cdot\mathbf{J}_1 \tag{10}$$

Where $\mathcal{X}_{1,\mathrm{EFIE}}$ and $\mathcal{R}_{1,\mathrm{EFIE}}$ are the imaginary and real parts of $\mathcal{L}_{1,\mathrm{EFIE}}$, respectively; $\lambda$ and $\mathbf{J}_1$ are characteristic values (CVs) and currents, respectively.

The standard method of moment (MoM) is adopted for the discretization of the impedance operator $\mathcal{L}_{1,\mathrm{EFIE}}$ where the RWG (Rao-Wilton-Glisson) basis functions are used as the trial functions for $\mathbf{J}_1$, $\mathbf{J}_2$, and $\mathbf{M}_2$. Note that only RWGs are used hereby to yield correct solutions in the GIBC scheme (neither dual bases nor mixed testing with $\mathrm{RWGs}+\hat{n}\times\mathrm{RWGs}$ are used).

To iteratively solve for characteristic modes with ARnoldi PACKage (ARPACK), many operations $\mathcal{L}_{1,\mathrm{EFIE}}\cdot\mathbf{J}$ are to be computed. It is of note that operators $\mathcal{L}_{21}$, $\mathcal{L}_{12}$ and $\mathcal{K}_{12}$ in (9) are low-rank when the $S_1$ and $S_2$ are separated. Therefore, keeping $q$ terms in the truncated SVD for a given error tolerance, $\mathcal{L}_{21}$ can be approximated as

$$\mathcal{L}_{21}\approx\mathcal{U}\cdot\Sigma\cdot\mathcal{V}^{\dagger} \tag{11}$$

Usually, $q$ is much smaller than the number of RWGs on either $S_1$ or $S_2$. The truncated expression (10) can be efficiently obtained with the randomized SVD technique [5]. To accelerate MVPs $\mathcal{L}_{1,\mathrm{EFIE}}\cdot\mathbf{J}$, we solve $q$ scattering problems beforehand, which are embarrassingly parallelizable. These scattering problems are resulted from operations in the first $\{\bullet\}$ in (12)

$$\tilde{\mathcal{L}}_{22}^{-1}\cdot\mathcal{L}_{21}\cdot\mathbf{J}=\left\{\tilde{\mathcal{L}}_{22}^{-1}\cdot\mathcal{U}\cdot\Sigma\right\}\cdot\Sigma^{-1}\cdot\left\{\mathcal{U}^{\dagger}\cdot\mathcal{L}_{21}\cdot\mathbf{J}\right\} \tag{12}$$

where $\tilde{\mathcal{L}}_{22}=\mathcal{L}_{22}-\mathcal{K}_{22}\cdot\mathcal{Z}_2$. Operations in the second $\{\bullet\}$ can be computed cheaply with the discrete empirical interpolation method (DEIM) [6] as

$$\mathcal{U}^{\dagger}\cdot\mathcal{L}_{21}\cdot\mathbf{J}=\left([F]^T[U]\right)^{-1}\left([F]^T[L_{21}]\right)\{j\} \tag{13}$$

where $[U]$, $[L_{21}]$ and $\{j\}$ are the matrix or vector representations of $\mathcal{U}$, $\mathcal{L}_{21}$ and $\mathbf{J}$. $[F]$ is a matrix formed by several $q$ columns of an $N\times N$ identity matrix ($N$ is the number of RWGs on $S_1$), where the column indices are generated by DEIM. Other operations with $\mathcal{L}_{12}$ and $\mathcal{K}_{12}$ can be similarly conducted.

## 3. Numerical Results

The first example validates the reduced order model of NGF in (9). As shown in Figure 2, a pair of cavities coupled by an aperture is modeled with FEM, where

around 60,000 edge elements are generated in the interior volume of the cavities. The dielectric constants for both cylinders are $\varepsilon_r = 4$. We only use 20 solenoidal modes in (5), and compute the error between $[K]^{-1}(k)\{v\}$ and $[K]_R^{-1}(k)\{v\}$, where $\{v\}$ is a random vector, and $[K]^{-1}(k)\{v\}$ is computed with conventional iterative solvers, e.g., GMRES. With a frequency sweeping, we compare the error in Fig. 3, where good agreement is observed. In addition, the CPU time for $[K]_R^{-1}(k)\{v\}$ is almost negligible, as the model complexity is significantly reduced by the reduced modal representation.

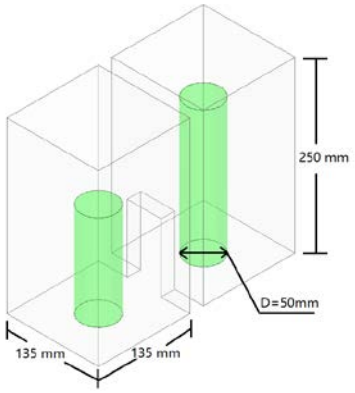


**Figure 2**. Aperture-coupled cavity pair loaded with dielectric cylinders.

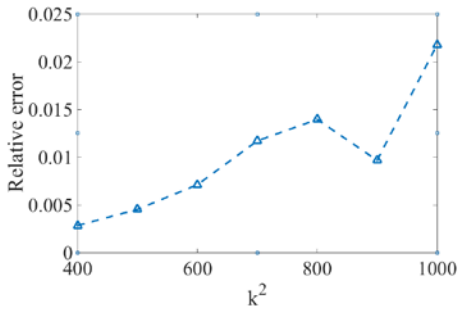


**Figure 3**. Error of reduced modal representation of NGF.

The second example performs CMA of a conducting sphere placed on top of a dielectric block (background inhomogeneity). The geometry is illustrated in Fig. 4, where the distance between the sphere and the block is $0.1\lambda$, and the dielectric constant of the block is $\varepsilon_r = 4$.

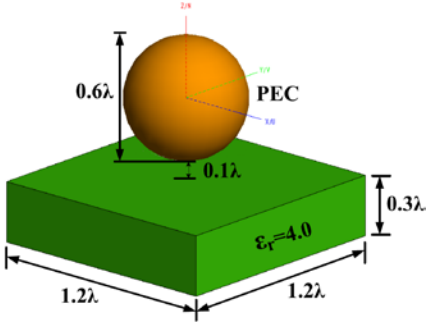


**Figure 4**. A conducting sphere on top of a dielectric block.

The model contains 525 RWGs on $S_1$ and about 2,300 RWGs on $S_2$. When the first 100 singular values and vectors are used, the truncated SVD yields 1% error in the approximation of $\mathcal{L}_{21}$. Fewer singular values are required when the sphere and block are further separated. In this simulation, 50 solenoidal modes are used in (5), and $\mathcal{L}_{1,\mathrm{EFIE}} \cdot \mathbf{J}$ is computed in a few seconds by the proposed scheme. As shown in Figs. 5, modal currents of the first two characteristic modes (CMs) are plotted. Note that when no dielectric block exists, these two CMs are degenerate. They have the same current pattern but different orientations. However, when the dielectric block is present, the degeneracy is broken, where the second modal current is modified [Fig. 5(b)], while the first modal current remains the same due to the geometrical symmetry [Fig. 5(a)].

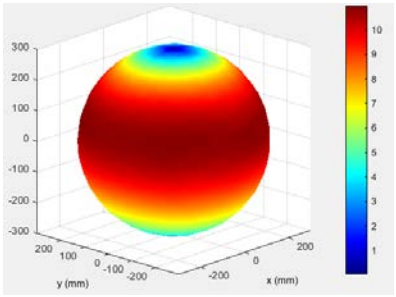


**Figure 5(a)**. Modal current of the first CM, characteristic value=1.172.

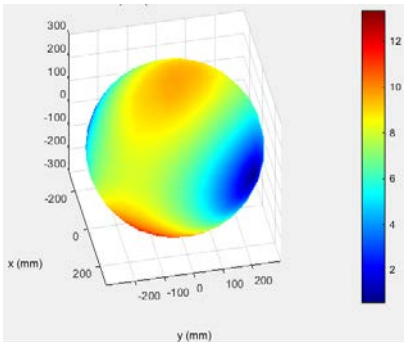


**Figure 5(b)**. Modal current of the second CM, characteristic value=1.179.

The third example demonstrates the synthesis of RCS in inhomogeneous electromagnetic environment. As shown in Fig. 6(a), a conducting loop is placed near the inhomogeneity, namely a human head shaped dielectric. The operating frequency and the relative permittivity of the dielectric are set to 800 MHz and 4.0, respectively. In this simulation, the model contains 352 triangles on the loop, and 5,322 triangles and 58,076 tetrahedra in the head shaped dielectric. The radiation pattern of the first CM of the loop computed with NGF is illustrated in Fig. 7(a). As a comparison, we plot in Fig. 7(b) the radiation pattern of the first CM without the presence of the head shaped dielectric. We further study the scattering of the entire system where an incident plane wave propagating in $-\hat{x}$ direction and polarized along $\hat{y}$ -axis is introduced. The RCS results computed by a finite-element boundary-integral (FE-BI) scheme and the NGF scheme

[7] are compared in Fig. 8, where good agreement is observed. Furthermore, we reconstruct the RCS using 10 characteristic modes, which agrees well with the directly computed results.

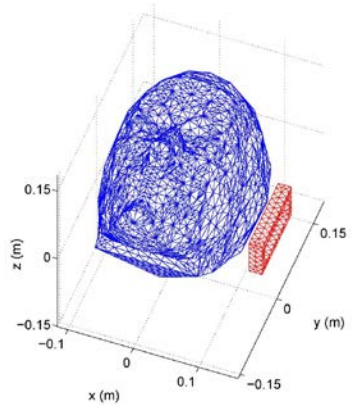


**Figure 6**. A loop (red) placed by a head shaped dielectric (blue).

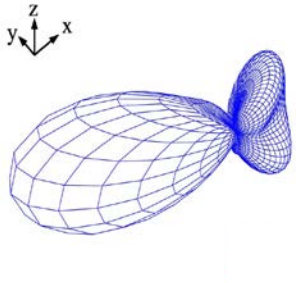


**Figure 7(a)**. Radiation pattern of the first loop CM when the head shaped dielectric is present.

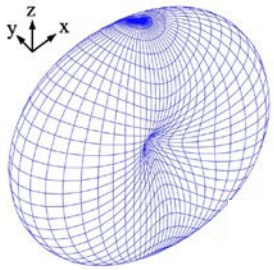


**Figure 7(b)**. Radiation pattern of the first loop CM when no head shaped dielectric exists.

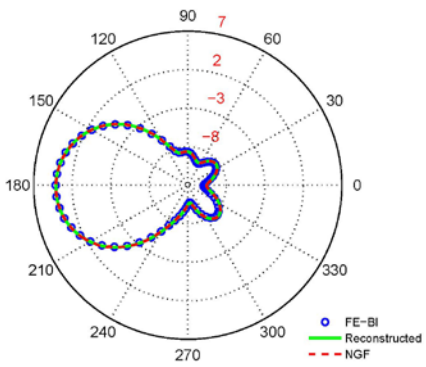


**Figure 8**. Comparison of computed RCSs.

## 4. Conclusion

Characteristic mode analysis for objects immersed in inhomogeneous electromagnetic environment is enhanced by reduced order models of background inhomogeneities. Our scheme significantly reduces the model complexities by reduced modal representation of the numerical Green's function. The model order in the object-background interaction is further reduced by the low-rank randomized singular value decomposition and the discrete empirical interpolation method. Synthesis of radar cross section in inhomogeneous environment is feasible with a small number of characteristic modes. Examples with higher complexities and more computational detail will be discussed in the conference.

## 5. Acknowledgements

This work was supported in part by the National Science Foundation under Award Number 1218552, and in part by the seed project No. 1508 by Temasek Laboratories at National University of Singapore.

## 6. References

1. R. J. Garbacz and R. H. Turpin, "A generalized expansion for radiated and scattered fields," IEEE Trans. Antennas Propag., vol. 19, pp. 348–358, 1971.

2. R. F. Harrington and J. R. Mautz, "Theory of characteristic modes for conducting bodies," IEEE Trans. Antennas Propag., vol. 19, pp. 622–628, 1971.

3. M. Cabedo-Fabres, Systematic design of antennas using the theory of characteristic modes [Ph.D. thesis]. Univ. Politecnica de Valencia, Spain, 2007.

4. Tsang, L. and S. Huang, "Broadband Green's function with low wavenumber extraction for arbitrary shaped waveguide and applications to modeling of vias in finite power/ground plane," Progress In Electromagnetic Research, Vol. 152, 105–125, 2015.

5. N. Halko, P. G. Martinsson, and J. A. Tropp, "Finding structure with randomness: Probabilistic algorithms for constructing approximate matrix decompositions," SIAM Rev. vol. 53, no. 2, pp. 217–288, 2011.

6. A. Hochman, J. F. Villena, A. G. Polimeridis, L. M. Silveira, J. K. White and L. Daniel, "Reduced-Order Models for Electromagnetic Scattering Problems," *IEEE Trans. Antennas Propag.*, vol. 62, no. 6, pp. 3150-3162, June 2014.

7. I. Dai, H. Gan, W. C. Chew, and C. Wang, "Characteristic Mode Analysis Using Green's Function of Arbitrary Background," IEEE International Symposium on Antennas and Propagation and USNC-URSI National Radio Science Meeting, Puerto Rico, Jun., 2016.